

## Research on Subwavelength Microphotonic Sensors for In-situ Monitoring with High Spatial and Temporal Resolution in Manufacturing Environments

**Xiaochun Li**

University of Wisconsin-Madison

**Chee Wei Wong**

Columbia University

**David Dornfeld**

University of California, Berkeley

**Brian Thomas**

University of Illinois, Urbana-Champaign

**Abstract:** Micron-sized subwavelength structured photonic sensors could allow critical thermo-mechanical phenomena in manufacturing processes to be monitored, while offering tremendous advantages. To implement these novel sensors into real manufacturing processes, the microring sensors can be embedded at critical locations in metallic structures, which are heavily used in hostile manufacturing environments. This paper presents our research progress on fabrication, embedding, and application of integrated microring sensors. For fundamental study, microring resonators have been microfabricated on-chip with silicon-on-insulator wafer substrates. The fabricated optical resonators offer Qs on the order of 20,000, enabling significantly improved temporal sensing and detection of high-frequency strain variation. A new approach to fabricate metal embedded photonic structures was developed. Various thin film photonic materials were studied for embedded microphotonic sensors. Effect of process parameters on refractive index of silicon nitride/silicon oxynitride films was studied. Issues on design and implementation of micro sensors for Chemical Mechanical Planarization (CMP) were studied and a grafting process was designed to embed micro sensors into polishing pads. A preliminary design for the sensor and its installation into a continuous casting mold was also developed.

### 1. Introduction

Recent developments in integrated microphotonic have led to unprecedented potential towards robust sensor enhancements for manufacturing systems.

These micron-sized subwavelength structured photonic sensors, e.g. microring and photonic crystal resonators, could allow critical thermo-mechanical phenomena in manufacturing processes to be monitored, while offering immunity to electromagnetic interference, resistance to hostile environments, multiplexing capabilities, and extremely high rates of data collection. Owing to their small sizes, distributed microphotonic sensors could be incorporated into mechanical structures without interfering with normal operation of the piece. The small size of these sensors enables them to respond to environmental changes (strain, thermal and vibrational) much more quickly than ordinary macro-sensors. In addition they permit data to be obtained with greatly enhanced spatial resolution and sensitivity.

Recent advances in photonic device microfabrication have made it possible to construct very small microring resonators in a variety of materials, including glass [1], polymers [2], silicon [3], silicon nitride ( $\text{Si}_3\text{NH}_4$ ) [4], silicon oxynitride ( $\text{SiON}$ ) [5], and III-V semiconductors [6]. The change in the resonant frequency  $\Delta\lambda$  with respect to applied strain  $\varepsilon$  is related as:  $\Delta\lambda/\lambda_0 = n_{\text{eff}} [1 - \frac{1}{2} \wp(\varepsilon) n_{\text{eff}}^3] \varepsilon$  (1),

where  $\lambda_0$  is the resonant frequency,  $n_{\text{eff}}$  an effective refractive index,  $\wp(\varepsilon)$  the photoelastic coefficient as a function of strain. For strains on order 0.1%, the photoelastic correction term can be negligible, and the change in resonant frequency  $\Delta\lambda$  is a linear function of strain  $\varepsilon$ . We also note here that  $(\Delta\lambda/\lambda_0)$  is a linear function of temperature variations, and

related as:  $\Delta\lambda/\lambda_0 = n_{\text{eff}} (\alpha+\beta) \Delta T/T$ , where  $\alpha$  is the linear thermal expansion coefficient and  $\beta$  the photothermal coefficient expressing dependence of refractive index on temperature. For a given signal-to-noise limit in tracking motion of a Lorentzian peak, therefore, the strain sensitivity of microring resonators to external strain perturbation is identified by  $Q (= \lambda_0/\delta\lambda)$ . For example, if one conservatively assumes a 3-dB differentiation limit between two overlapping Lorentzian peaks, the resolution in strain detection is proportional to  $\delta\lambda$  or equivalent to  $\lambda_0/Q$ . Combining with Equation (1), this gives a strain resolution as proportional to  $1/Q$ : that is, a larger  $Q$  gives a better strain resolution. Microring resonators, in high-index contrast silicon material systems, have reported  $Q$  on order 8,000, and up to even 57,000 [7].

To implement these novel sensors into real manufacturing processes, the microring sensors must survive hostile environments and provide high accuracy, long-term stability, and good reliability during service. To achieve this goal, distributed microring sensors can be embedded---thus avoiding direct exposure from external manufacturing environments (e.g. chemicals, moisture, contamination etc.)---at critical locations but without interfering with normal operation of the structure. The small size of these sensors will permit data to be obtained with significantly enhanced spatial and temporal resolution as well as superior sensitivity. Challenges for microring sensor embedding arise from the fact that most structures used in hostile manufacturing environments are metallic. It is necessary to fabricate and embed microphotonic sensors into metal wafers before the sensors can be implemented. SiO<sub>2</sub>-based Fiber Bragg Grating (FBG) sensors have been successfully embedded into nickel and stainless steel for temperature and strain measurements in laser-based manufacturing [8-12]. Moreover, micro optical thin films are expected to demonstrate much superior properties than their macro optic counterparts, e.g. amorphous micro/nano SiO<sub>2</sub> and Si<sub>3</sub>N<sub>4</sub> thin films actually have significantly higher strain limit (3~10%) than that of most metals (0.2~1%) [13]. Thus, it is promising to fabricate metal embedded microphotonic sensors that can withstand the hostile manufacturing environments.

The successful implementation of these embedded microphotonic sensor arrays could advance the fundamental understanding of manufacturing processes, thus significantly improving productivity and generating significant cost savings. To date, a systematic study of these subwavelength microphotonic sensors for strain and temperature measurements has yet to be conducted that would

allow the potential of these devices to be fully harnessed for manufacturing processes. This paper presents our research progress on integrated subwavelength photonic sensors that offers exciting new opportunities for fundamental understanding and better control of manufacturing processes.

## 2. Fundamental study on microring resonators for high spatial and temporal resolution strain sensors

Microring resonators have been microfabricated on-chip with silicon-on-insulator wafer substrates (hence permitting CMOS-level batch processing) and each chip packaged to signal (input) and detector single-mode optical fibers.

In the development of high-performance microphotonic sensors, the traveling wave microring resonator (on order several micrometers) is one of the critical elements towards high strain sensitivity, high spatial resolution and short temporal resolution. The strain sensitivity is dependent on the spectral linewidth of the microphotonic resonator – our focus is to develop high-quality factor optical resonators and with oxide, nitride, oxynitride material systems for embedding in metals to enhance sensor reliability (see Fig. 1). In addition, we investigate numerically the optical coupling efficiency from designed gratings into the optical waveguides.

Microring resonators (such as studied in our group, as shown in Fig. 1) are traveling wave resonators with the transmission response following a Lorentzian line shape filter. The microring becomes a resonant sink for the signal power when an integral number of wavelengths match its optical circumference. A characteristic of microring resonators is the quality factor  $Q$ : a measure of its extrinsic and intrinsic losses, a measure of its detection sensitivity for localized strain (thermal or mechanical) sensing, and a measure of the ultimate response time (continuous strain event monitoring) of these sensors.  $Q$  is defined as  $\lambda_0/\delta\lambda$ , the ratio of the resonator operating wavelength  $\lambda_0$  to the resonator full-width half-maximum (FWHM)  $\delta\lambda$ . The resonance will be tracked to determine the external strain on the microring sensors. The resonant spectral modes are illustrated in Fig. 2, through the discrete Fourier transform of a temporal pulse in the resonator. The numerical simulations (a few to several hours on cluster or stand-alone machines) are performed in RSoft FullWave, a finite-difference time-domain solver of Maxwell's equations.

Recent developments on optical resonators in our group have experimentally measured loaded  $Q$ s on

order 20,000 – two to three orders of magnitude better than conventional fiber Bragg sensors. This is illustrated in Fig. 3. Using optical fiber input and output coupling to the resonators, speed of light data transmission is obtained between the individual sensors and the data collection endpoints in the sensor network. This permits significantly improved

temporal sensing and detection of high-frequency strain variation, supported even with commercial off-the-shelf photodetectors through wavelength-division multiplexing. The small-sized resonators also permit spatial resolution at least two orders of magnitude better than conventional fiber Bragg sensors.

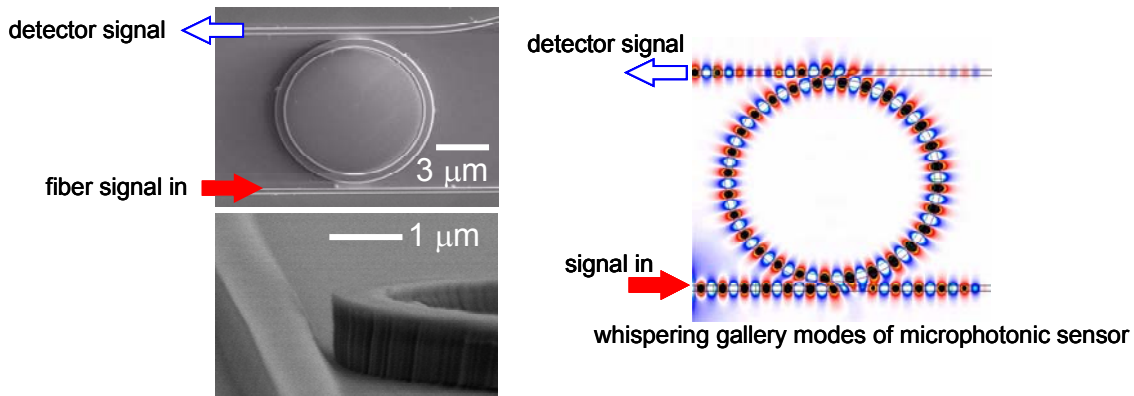


Figure 1. Microring optical sensors fabricated through the Columbia – Wisconsin Madison collaboration

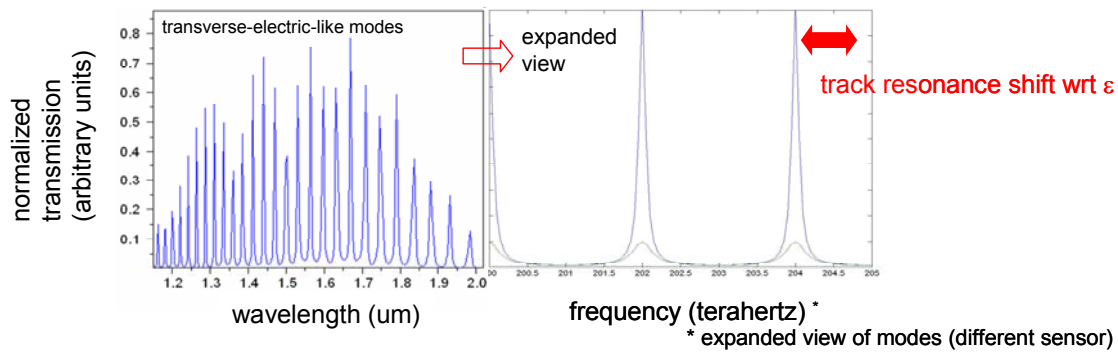


Figure 2. Numerical spectral of microring resonators

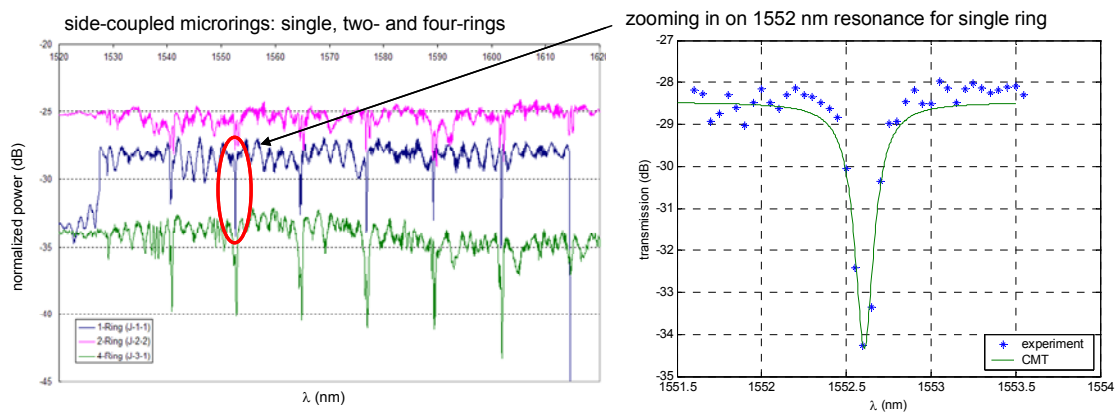


Figure 3. Experimentally measured resonances of microring sensors  
 Left panel: spectrum of resonators for 1,2 and 4 rings  
 Right panel: expanded view of measurement data with CMT theory comparison

### 3. Study on embedding of microring sensors in metals

Thin film photonic materials were studied and a novel batch fabrication technique was developed to embed microphotonic sensors into metal.

**3.1. Study on thin film photonic materials:** Since these sensors must operate in extremely hostile environments, particularly under long term high temperatures and stresses, the materials making up these sensors need to withstand such harsh conditions. Furthermore, the films should have good adhesion to metal substrates (e.g. nickel) to ensure sensors function well under elevated temperatures.

Silicon nitride and alumina are excellent photonic materials due to their superior thermal stability and well-matched coefficients of thermal expansion with metal substrates. 1 Thin film layers of alumina/silicon nitride/alumina/ nickel were annealed at 600 °C for 10 hours to investigate reliabilities of these photonic thin films under elevated temperature environment. Figure 4 (a) illustrates the thin film system before annealing. (b) is the result of Energy Dispersive Spectroscopy (EDS) line scan. The annealed thin film system and EDS line scan result are shown in Figure 5. No apparent interdiffusion and delamination between thin films were found in this experiment.

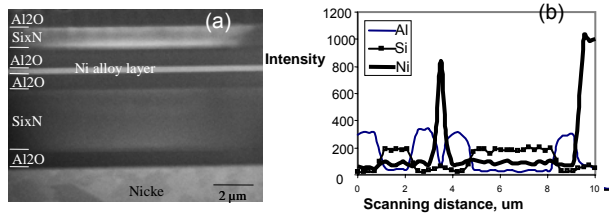


Figure 4. (a) Multi-layer thin film system before annealing, (b) EDS line scan result of thin film system.

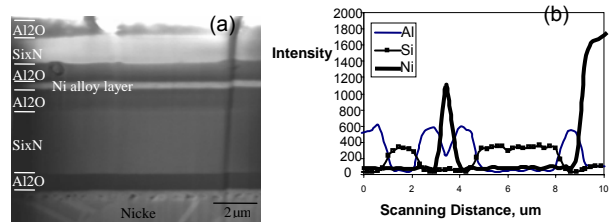


Figure 5. (a) Multi-layer thin film system after annealing, (b) EDS line scan result of thin film system.

Generally, a passive photonic device comprises two kinds of material with certain reflective index (n) contrast. The lower n material is used as clad, and the one with higher n is used as core for guiding light. In this study silicon dioxide, which is widely used as cladding material, was selected as cladding material. Since alumina is prone to pinhole problem when

deposited by electron beam evaporator, plasma enhanced chemical vapor deposition (PECVD) silicon nitride/silicon oxynitride was selected as the core material. It should be noted the reflective index of PECVD silicon nitride/ silicon oxynitride can be adjusted by inputting different amount of gases and different type of gases. As shown in Figure 6, with different process condition listed in Table 1, the reflective index varies from silica to silicon rich silicon nitride.

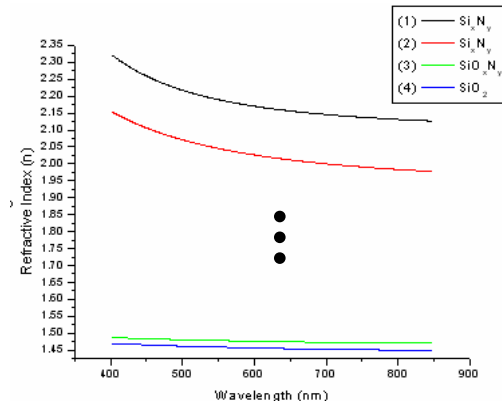


Figure 6. Reflective index varied with wavelength and process condition

**Table 1.** PECVD process condition

Material	SiH <sub>4</sub>	NH <sub>3</sub>	N <sub>2</sub>	NO <sub>2</sub>
1.Si <sub>x</sub> N <sub>y</sub>	10sccm	4sccm	1000sccm	-
2.Si <sub>x</sub> N <sub>y</sub>	8sccm	4sccm	1000sccm	-
3.SiO <sub>x</sub> N <sub>y</sub>	10sccm	4sccm	-	800sccm
4.SiO <sub>2</sub>	8.8sccm	-	-	1200sccm

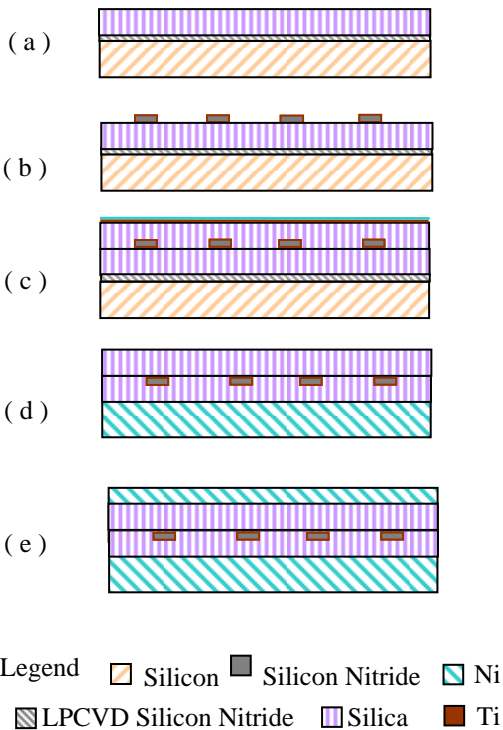
Base pressure: 0.5mTorr. Deposition temperature: 300°C. Power: 50W

### 3.2. Fabrication of metal embedded photonic structures

A new approach to fabricate metal embedded photonic structures based on standard microfabrication techniques and electroplating was developed, in which a batch of device fabricated on a silicon wafer were directly transferred and embedded into electroplated metals. Details of the fabrication are depicted in Figure 7.

A 3-inch silicon wafer was first thoroughly cleaned (degreased with Acetone / Isopropanol / DI water) followed by Piranha cleaning, which is comprised of hot sulfuric acid and hydrogen peroxide that are effective against organic contaminants, and buffed oxidize etching (6:1 solution). Then a thin layer of low stress silicon nitride (1.0 μm thick) was thermally grown by low pressure chemical vapor deposition (LPCVD) to serve as an etch stop layer for the subsequent KOH etching of the silicon wafer. The back side LPCVD silicon nitride of the silicon wafer was etched out by

reactive ion etching (RIE). On the top surface of the front side silicon nitride, silica was deposited as cladding layer. Figure 7(a) illustrates the structure at this point. Silicon nitride was then deposited by PECVD and patterned by lithography and RIE to form the core of device. Another silica layer was deposited to sandwich the core layer. To transfer the photonic structure from silicon to metal substrate, a thin layer of Ti (50nm) was sputtered as an adhesion-promoting layer, followed by a Ni seed layer (300nm). The structure was then electroplated to form a thick nickel layer (approximately 180  $\mu\text{m}$ ) on one side. After deposition, the silicon wafer was completely etched out in a 30% KOH solution at 80°C. Upon the complete removal of the etch stop, i.e. silicon nitride layer, by RIE, the structures were fully transferred to an electroplated Ni substrate from the Si wafer. Figure 8 shows the photonic structure (optical waveguide) on nickel substrate.



(a) Deposit silicon nitride on Si by LPCVD; dry etch the silicon nitride from back side; deposit silica by PECVD; (b) Depositions of silicon nitride by PECVD; perform lithography to get core layer pattern; (c) Deposit silica again; sputter Ti and Ni; (d) Electroplating Ni as substrate; transfer sensor structure to metal substrate; wet etch Si and dry etch LPCVD silicon nitride from Top; (e) Sputter Ti and Ni; electroplate Ni; embed the photonic structure into metal

Figure 7. Embedded photonic structure fabrication process

To embed these photonic structures into nickel, more fabrication steps were needed. Ti/Ni layers were again sputtered. Finally a thick nickel layer (e.g. 50 $\mu\text{m}$ ) was electroplated to encapsulate the devices. Figure 9 depicts the full embedded device.

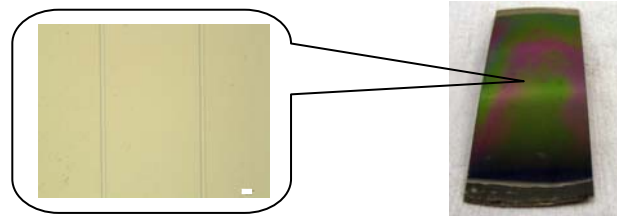


Figure 8. Photonic structure on metal substrate



Figure 9. Full embedded device

#### 4. Research progress on implementation of sensors for manufacturing processes

Two important manufacturing processes, Chemical Mechanical Planarization (CMP) [14,15] and Continuous Casting of steel [16], will be used as testbeds to test the novel high spatial, temporal and sensitivity resolution sensor in demanding manufacturing environments.

##### 4.1. Design and implementation of sensors for CMP

The integration of sensors in CMP will allow the progress of fundamental study and model development. In addition, sensors will enable real time manufacturing feedback for improved process monitoring and control. Despite the acceptance of CMP in IC manufacturing, there is little known of the CMP interface at the micro scale. The only sensors currently used in CMP are on the macro or machine scale. As seen in Table 2, machine level sensors are most prominently used for end point detection via optical sensors and motor current sensors. Pad and wafer embedded sensors allow for the characterization of many more aspects of the CMP process.

To reach the micro scale, sensors must be placed closer to the interface. There are two options, embedding sensors on the wafer or embedding sensors on the pad. Wafers can be embedded with micro contact pressure

sensors. Alternatively, sensors can be embedded into the pad. Both pad and wafer sensors have their own advantages.

Sensors in the wafer allow the highest resolution and will most accurately reflect interactions on the interface. However, since CMP is a destructive process, the wafer sensors will become miscalibrated after only a short time elapse and will eventually be destroyed completely. It would also be unlikely for sensors to be embedded on a production wafer which is to be used in an actual manufacturing process. Thus, sensors on wafers can only be used for fundamental study and model development in laboratory settings.

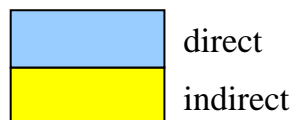
Sensors in the pad allow for real time manufacturing monitoring and control. Within Wafer Non Uniformity (WIWNU) is a large issue in fabrication facilities. It is

compensated with carrier head back pressure zone variation; however, current monitoring of WIWNU effects are measured ex situ. This lack of real time control loop not only slows the production process, it can decrease yields substantially. Pads embedded with sensors would allow for in situ real time control for optimal zone back pressure.

In addition to WIWNU detection, a sensor embedded pad could detect pad degradation and variation of pad degradation. The largest drawback of a pad embedded sensor is that asperity level resolution would not be possible. As seen in Figure 10, spatial resolution is a function of local sensor resolution and distance from surface. The exact sensitivity must be determined experimentally since pad material properties vary from pad to pad.

Table 2: Uses of sensors in the Pad, Wafer, and Machine

Sensor location used for	PAD	WAFER	Machine
In-situ monitoring of wafer to wafer pad degradation	<b>Thin Films, MEMS resonator</b>		<b>Acoustic Emission</b>
Monitoring spatial variation of pad degradation	<b>Thin Films, MEMS resonator</b>		<b>Acoustic Emission</b>
In-situ feed back control of head zone pressure	<b>Thin Films, MEMS resonator</b>		
Ex-situ head zone pressure optimization	<b>Thin Films, MEMS resonator</b>	<b>MEMS capacitance</b>	
In-situ scratch detection			<b>Acoustic Emission</b>
End point detection			<b>Motor current, Acoustic Emission</b>
			<b>Optical</b>
Ex-situ pattern effect characterization		<b>MEMS capacitance</b>	
Modeling parameter extraction & fundamental study	<b>Thin Films, MEMS resonator</b>	<b>MEMS capacitance</b>	



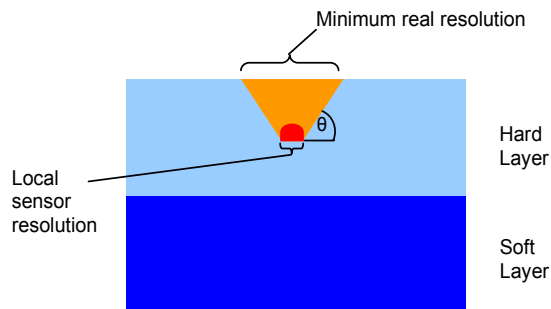


Figure 10. Schematic of an embedded sensor and effects of location on spatial resolution

Non destructive removal of pad sections has proven difficult. Thus, to remove the soft layer, we propose to remove the material on a mill. As seen in Figure 11, we can machine a 3 inch diameter blind hole into the back of the pad. With this method, we can customize the precise depth of the hole. The 3 inch sensor array will be imbedded directly onto the backside of the hard layer. In our lab, we have access to 30 inch pads which are oversized for our GNP CMP machine. We can graft a 3 inch diameter section from the unused portion of the pad and use it as the soft layer. The grafting from the same pad is necessary due to inconsistencies in material from pad to pad. Subtleties such as storage humidity or date of manufacture can alter pad hardness modulus.

The actual grafting process can be seen in Figure 12. The cross section is show in 3 steps: machining the soft layer, machining the hard layer, and grafting the two together with the sensor at the interface. With this

process, the depth of sensor in the pad can be chosen. For example, the sensor can be half way into the hard layer or just at the interface.

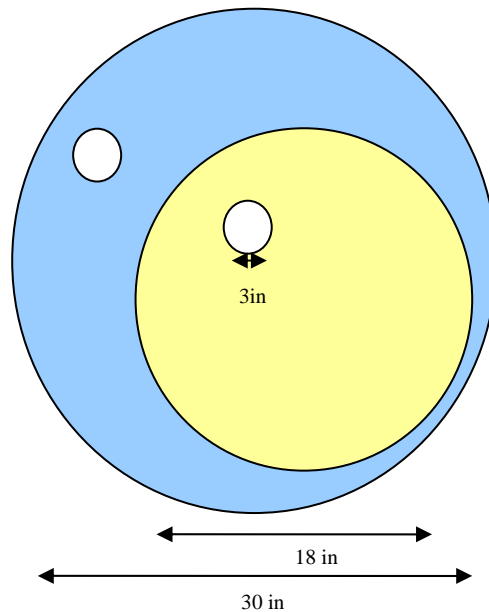


Figure 11. The blue colored circle represents a commercially available 30 inch pad. The yellow colored circle represents the 18 inch diameter pad necessary for the GNP machine at UC Berkeley. The white circles represent the machined sensor location and the grafted section.

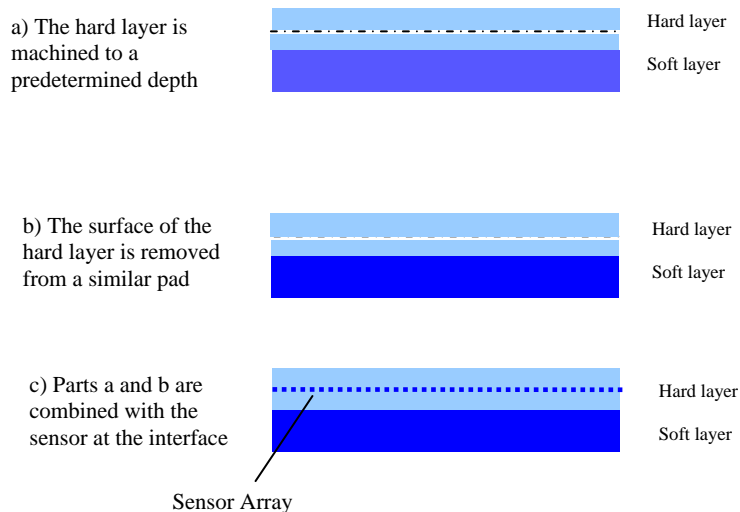


Figure 12: Grafting process cross section. As shown, the sensor is half way into the hard layer.

#### 4.2 Mold sensor design for Continuous-Casting

This part of the project aims to develop and validate the new type of in-mold sensor for use in the commercial continuous casting of steel. A preliminary design for the sensor and its installation into a continuous casting mold is depicted in Figure 13. A key feature of this design is that the sensor will monitor temperature very near to the hotface of the steel at the meniscus, which is the most crucial part of the process. Conventional thermocouples experience severe damping of the temperature signal by the thick (12-mm) copper mold between the solidifying steel and the thermocouple. Improved versions of the sensor-strip design and manufacturing process are being developed through collaborations between the University of Illinois, where the sensor design, modeling, testing, evaluation and implementation is being coordinated, the University of Wisconsin-Madison, where the sensor strip will be

fabricated, a commercial mold manufacturer, where the strip will be attached to a commercial mold, and a commercial steel company, where the mold and sensor will be tested in service. The sensor strip will be attached to the mold, and coordinated or integrated with the electroplating process used to apply the nickel coating layer. The feasibility of the design has been approved by the mold manufacturer, pending the outcome of several lab-scale tests, which are currently being conducted. These tests involve attaching prototype sensor strips to copper pieces, dipping the assembly into molten steel for a time chosen to approximate the temperature distribution expected under continuous casting conditions, and performing metallography to determine the integrity of the bond, and accuracy of the sensor, relative to conventional thermocouples.

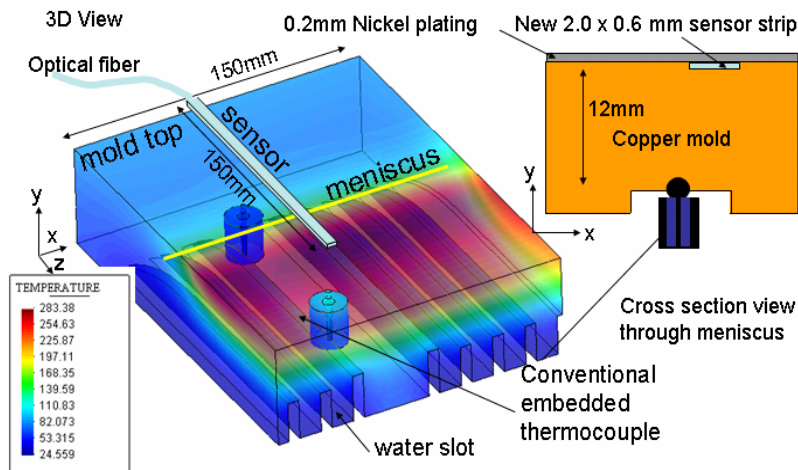


Fig.13. Sensor strip bonded into narrow face of casting mold

#### 5. Summary

Integrated microphotronics have unprecedented potential for sensor enhancements for manufacturing applications. These micron-sized photonic sensors could allow critical thermo-mechanical phenomena in manufacturing processes to be monitored, while offering immunity to electromagnetic interference, resistance to hostile environments, multiplexing capabilities, and extremely high rates of data collection. Recent advances in photonic device microfabrication have made it possible to construct very small microring resonators in a variety of materials. This paper presents our research progress on integrated subwavelength photonic sensors that offers exciting new opportunities

for fundamental understanding and better control of manufacturing processes.

For fundamental study, microring resonators have been microfabricated on-chip with silicon-on-insulator wafer substrates. The fabricated optical resonators offer  $Q$ s on the order of 20,000, enabling significantly improved temporal sensing and detection of high-frequency strain variation. The small-sized resonators also permit spatial resolution at least two orders of magnitude better than conventional fiber Bragg sensors.

A new approach to fabricate metal embedded photonic structures based on standard microfabrication

techniques and electroplating was developed, in which a batch of device fabricated on a silicon wafer were directly transferred and embedded into electroplated metals. Various thin film photonic materials were studied for embedded microphotonic sensors. Thin film photonic layers of alumina and silicon nitride/alumina/nickel were annealed at 600 °C for 10 hours and no apparent interdiffusion and delamination between thin films were found. Effect of process parameters on refractive index of silicon nitride/silicon oxynitride films was studied.

Issues on design and implementation of micro sensors for Chemical Mechanical Planarization (CMP) were studied and a grafting process was designed to embed micro sensors into polishing pads. A preliminary design for the sensor and its installation into a continuous casting mold was also developed. A key feature of this design is that the sensor will monitor temperature very near to the hotface of the steel at the meniscus, which is the most crucial part of the process. Improved versions of the sensor-strip design and manufacturing process are being developed through collaborations.

## 6. Acknowledgements

This work is supported by the National Science Foundation under Grant # DMI 0528668.

## 7. References

- [1] S.T. Chu et al., "An 8-channel add/drop filter using vertically coupled microring resonators over a cross-grid," *Photonics Technol. Lett.*, 11, 691-693, 1999.
- [2] P. Rabiei et al., "Polymer micro-ring filters and modulators," *J. of Lightwave Technol.*, 20, 1968-1975, 2002.
- [3] B. E. Little et al., "Ultra-compact Si-SiO<sub>2</sub> microring resonator optical channel dropping filters," *Photonics Technol. Lett.*, 10, 549-551, 1998.
- [4] D. J. W. Klunder, "Vertically and laterally waveguide-coupled cylindrical microresonators in Si<sub>3</sub>N<sub>4</sub> on SiO<sub>2</sub> technology," *Appl. Phys. B* 73, 603-608, 2001
- [5] A. Melloni et al., "Ring-resonator filters in silicon oxynitride technology for dense wavelength-division multiplexing systems," *Opt. Lett.*, 28, 1567-1569, 2003.
- [6] D. Rafizadeh, "Waveguide-coupled AlGaAs/GaAs microcavity ring and disk resonators with high finesse and 21.6 nm free spectral range," *Opt. Lett.*, 22, 1244-1246, 1997
- [7] T. Baehr-Jones, M. Hochberg, C. Walker, and A. Scherer, "High-Q ring resonators in thin silicon-on-insulator," *Appl. Phys. Lett.* 85, 3346 – 3347, 2004.
- [8] X.C. Li, A. Golnas, and F. Prinz, "Shape Deposition Manufacturing of Smart Metallic Structures with Embedded Sensors", *Proceedings of SPIE - The International Society for Optical Engineering*, v.3986, 2000, pp.160-171.
- [9] X.C. Li and F. Prinz, "Metal Embedded Fiber Optic Sensors for Layered Manufacturing Process Monitoring", *Journal of Manufacturing Science and Engineering*, Volume 125, Issue 3, 2003, pp. 577-585.
- [10] X. Li, J. Johnsen, J. Groza, and F. Prinz, "Processing and Microstructures of Fiber Bragg Grating Sensors Embedded in Stainless Steel", *Metallurgical and Materials Transactions*, vol.33A, September 2002, p.3019.
- [11] X. C. Li, F. Prinz, and J. Seim, "Thermal Behavior of Metal Embedded Fiber Bragg Grating Sensor", *Journal of Smart Materials and Structures*, no.10, 2001, pp.575-579.
- [12] X. Li and F. Prinz, "Embedded Fiber Bragg Grating Sensors in Polymer Structures Fabricated by Layered Manufacturing", *Journal of Manufacturing Processes*, vol. 5 No.1, 2003, pp. 78-86.
- [13] B. Halg, "On a Nonvolatile Memory Cell Based on Micro-Electro-Mechanics", *Electro Mechanical Systems Workshop*, Napa Valley, California, 172-176, 1990.
- [14] DeJule, R., "CMP Challenges Below a Quarter Micron," *Semiconductor International*, pp. 54-60 (Nov. 1997)
- [15] Feeney, P., et al, "Innovation in Traditional CMP Applications," *Proc. CMP-MIC Conference*, Fremont, CA, 2005, pp. 542-546
- [16] B.G. Thomas, "Continuous Casting," in *The Encyclopedia of Materials: Science and Technology*, Vol. 2, K.H. J. Buschow, R. Cahn, M. Flemings, B. Iilschner, E. J. Kramer, S. Mahajan and D. Apelian, eds., Elsevier Science Ltd., Oxford, UK., 2001, 1595-1599